



# Large Time Step Scheme Behaviour with Different Entropy Fix

Ihtram ul Haq<sup>1\*</sup>, Mukkarum Hussain<sup>2</sup>, Muhammad Jawed Iqbal<sup>1</sup>, and  
Noor Fatima Siddiqui<sup>3</sup>

<sup>1</sup> Institute of Space and Planetary Astrophysics, University of Karachi, Karachi, Pakistan

<sup>2</sup> Institute of Space Technology, Karachi, Pakistan

<sup>3</sup> Department of Mathematics, University of Karachi, Karachi, Pakistan

**Abstract:** The progress of numerical techniques for scalar and one dimensional Euler equation has been a great interest of researchers in the field of CFD for decades. In 1986, Harten developed a high resolution and efficient large time step (LTS) explicit scheme for scalar problems. Computation of nonlinear wave equation depicts that Harten's LTS scheme is a high resolution and efficient scheme. However, computations of hyperbolic conservation laws show some spurious oscillations in the vicinities of discontinuities for larger values of CFL. Zhan Sen Qian investigated this issue and suggested to perform the inverse characteristic transformations by using the local right eigenvector matrix at each cell interface location to overcome these spurious oscillations. Harten and Qian both used Roe's approximate Riemann solver which has less artificial viscosity than exact method at sonic points. The reduced artificial viscosity reduces the accuracy of Roe's method at sonic points. Roe's approximate Riemann solver cannot capture the finite spread of expansion fans due to the inadequate artificial viscosity at expansive sonic points. As a consequence of this expansion shocks that are nonphysical may occur. The existence of the expansion shock is said to violate the entropy condition. A variety of entropy fix formulae for Roe scheme have been addressed in the literature. In present work large time step total variation diminishing (LTS TVD) scheme developed by Harten and improved by Qian have been tested with different entropy fix and its effect has been investigated. Computed results are analyzed for merits and shortcomings of different entropy fix with large time step schemes.

**Keywords:** CFL restriction, explicit scheme, inverse shock, Shock tube problem, SOD, TVD scheme, 1D Euler equation

## 1. INTRODUCTION

The transient 1D Euler equation is hyperbolic, no matter whether the flow is locally subsonic or supersonic. The marching direction for 1D Euler equation is the time direction. Methods to solve hyperbolic system of equations are primarily derived for non-linear wave equation and then implemented on hyperbolic system of equations. Lax in 1954, modified Euler's Forward Time Central Space (FTCS) method and presented first-order accurate method to solve nonlinear wave equation. Lax method is stable for Courant-Friedrichs-Lewy (CFL) condition less than 1 and predicts the location of moving discontinuity correctly [1-2]. This method is very dissipative and smears discontinuities over several mesh points and become worse as CFL decreases. Lax-Wendroff proposed a second-order accurate method for non-linear wave equation. His method sharply defined discontinuity and also stable for CFL less than 1 but produce undesirable oscillations when discontinuities are encountered. Similar to Lax method quality of results computed by Lax-Wendroff method degrade as CFL decrease.

Lax and Lax-Wendroff central finite difference schemes are stable and converge if flow field is sufficiently smooth but produce unwanted oscillations when discontinuities are met. It is due to the fact that series expansion for obtaining a difference approximation is only valid for continuous functions and

has continuous derivatives at least through the order of difference approximation [1] [3]. Godunov recognized this deficiency and proposed a finite volume scheme instead of a finite difference scheme to avoid the need of differentiability. He used exact Riemann problem solution for evaluating the flux term at the cell interface. Computation of nonlinear wave equation is easily accomplished by using Godunov method but this method is very inefficient and take long time when applied to system of equations [4-6]. To overcome this problem Roe suggested solving linear problem instead of actual nonlinear problem [7]. Roe's approximate Riemann solver is efficient but cannot distinguish between expansion shock and compression shock. This is due to the violation of entropy condition and hence expansion shocks that are nonphysical may occur in computed results [8-9]. A number of entropy fix have been recommended in literature to overcome this problem. Roe's upwind approximate Riemann solver capture physics in more appropriate way than Lax and Lax-Wendroff central schemes but is only first order accurate. Like second order central methods, higher order upwind methods have the same deficiencies and produce undesirable oscillations when discontinuities are encountered [9-10].

Harten introduced the concept of Total Variation Diminishing (TVD) scheme. TVD schemes are monotonicity preserving schemes and therefore it must not create local extrema and the value of an existing local minimum must be non-decreasing and that of a local maximum must be non-increasing [10-12]. He worked on non-oscillatory first order accurate scheme and modified its flux function to obtain a second order accurate TVD explicit difference schemes for scalar and system of hyperbolic conservation laws. Numerical dissipation terms in TVD methods are nonlinear. The quantity varies from one grid point to another and usually consists of automatic feedback mechanisms to control the amount of numerical dissipation. After this break through a number of TVD scheme have been proposed and discussed in literature [13-17].

Stability criteria for explicit formulation limits time stepping and thus increase computational cost. Similar to previously discussed schemes, explicit formulation of Harten and other TVD schemes are also stable only for CFL less than 1. It is a challenging task to develop an explicit scheme which is stable for higher values of CFL number. In literature this kind of schemes are known as large time step (LTS) schemes and an active field of research for last three decades. Leveque described a method for approximating nonlinear interactions linearly which allows Godunov's method to be applied with arbitrarily large time steps [18-19]. Harten extended Leveque work and proposed second-order accurate LTS TVD explicit schemes for the computation of hyperbolic conservation laws. Computation of nonlinear wave equation depicts that Harten's LTS scheme is a high resolution and efficient scheme [20]. However, computation of system of hyperbolic conservation laws show some spurious oscillations in the vicinities of discontinuities when  $CFL > 1$ . Zhan Sen Qian worked on Harten LTS TVD scheme and observed that these spurious oscillations are due to the numerical formulation of the characteristic transformation used by Harten for extending the method for hyperbolic conservation laws [21-23]. Zhan Sen Qian showed that if the inverse characteristic transformations are performed by using the local right eigenvector matrix at each cell interface location then these spurious oscillations are eliminated. His computations for shock tube problem confirm that the modified large time step total variation diminishing (MLTS TVD) scheme eliminate spurious oscillations for system of hyperbolic conservation laws without increasing the entropy fixing parameter.

Harten and Qian both used Roe's approximate Riemann solver which has less artificial viscosity than exact method at sonic points. Roe's approximate Riemann solver differs from Godunov's exact Riemann solver only at sonic points. Roe's method has less artificial viscosity than Godunov's method at sonic points. The reduced artificial viscosity reduces the accuracy of Roe's method at sonic points. Roe's approximate Riemann solver cannot capture the finite spread of expansion fans due to the inadequate artificial viscosity at expansive sonic points. As a consequence of this is that expansion shocks that are nonphysical may occur [7-8]. This nonphysical behavior is due to the fact that the scheme cannot distinguish between an expansion shock and a compression shock. Each is a valid solution for this formulation. The existence of the expansion shock is said to violate the entropy condition. In order to make this scheme to satisfy the entropy condition it must be properly modified, such a correction is usually designated as entropy fix. A variety of entropy fix formulae for the Roe scheme have been addressed in the literature. Most famous are due to Harten-Hyman and Hoffmann-Chiang [9-11].

In present work large time step scheme [22] behavior with different entropy fix has been investigated. Computed results are analyzed for merits and shortcomings of different entropy fix with large time step schemes. Shock tube problem is used for validation purpose. Reasons of attraction in this test case are availability of analytical solution and at the same time presence of complex flow features namely, expansion, shock wave, and contact discontinuities.

## 2. NUMERICAL METHOD

1D Euler equation in conservation form is used in present study. Detail about governing equations and numerical method is given below:

$$\frac{\partial U}{\partial t} + \frac{\partial F}{\partial x} = 0 \quad (1)$$

$$\frac{\partial U}{\partial t} + A \frac{\partial U}{\partial x} = 0 \quad (2)$$

$$\text{where; } U = \begin{bmatrix} \rho \\ \rho u \\ \rho E \end{bmatrix} ; \quad F = \begin{bmatrix} \rho u \\ \rho u^2 + p \\ (\rho E + p)u \end{bmatrix} \quad (3)$$

$$A = \frac{\partial F}{\partial U} = \begin{bmatrix} 0 & 1 & 0 \\ (\gamma - 3)\frac{u^2}{2} & (3 - \gamma) & (\gamma - 1) \\ (\gamma - 1)u^3 - \gamma u E & -\frac{3}{2}(\gamma - 1)u^2 + \gamma E & \gamma u \end{bmatrix} \quad (4)$$

equation (1) in numerical flux form can be written as:

$$U_i^{n+1} = U_i^n - \lambda \left( f_{i+\frac{1}{2}}^n - f_{i-\frac{1}{2}}^n \right) ; \quad \lambda = \frac{\Delta t}{\Delta x} \quad (5)$$

The numerical flux for Qian's modified LTS TVD is given by:

$$f_{i+\frac{1}{2}} = \frac{1}{2} [F_{i+1} + F_i] + \left[ \frac{1}{2\lambda} \sum_{k=1}^m R_{i+\frac{1}{2}}^k (g_{i+1}^k + g_i^k) - \frac{1}{\lambda} \sum_{l=-K+1}^{K-1} \left\{ \sum_{k=1}^m R_{i+l+\frac{1}{2}}^k C_l (v^k + \beta^k)_{i+l+\frac{1}{2}} \alpha_{i+l+\frac{1}{2}}^k \right\} \right] \quad (6)$$

$$\text{where; } v_{i+\frac{1}{2}}^k = \lambda a_{i+\frac{1}{2}}^k ; \quad a = u, u + c, u - c \quad (7)$$

$$\beta_{i+\frac{1}{2}}^k = \begin{cases} \frac{(g_{i+1}^k - g_i^k)}{\alpha_{i+\frac{1}{2}}^k}, & \text{for } \alpha_{i+\frac{1}{2}}^k \neq 0 \\ 0, & \text{for } \alpha_{i+\frac{1}{2}}^k = 0 \end{cases} \quad (8)$$

$$\alpha_{i+\frac{1}{2}}^k = R^{-1} \Delta_{i+\frac{1}{2}} U \quad (9)$$

$$\sigma_{i+\frac{1}{2}}^k = \frac{K}{2} \left[ \psi \left( \frac{v_{i+\frac{1}{2}}^k}{K} \right) \left\{ 1 + \frac{K-1}{2} \psi \left( \frac{v_{i+\frac{1}{2}}^k}{K} \right) \right\} - \frac{K+1}{2} \left( \frac{v_{i+\frac{1}{2}}^k}{K} \right)^2 \right] \quad (10)$$

$$C_{\pm k}(v) = \begin{cases} c_k(\mu_{\mp}(v)), & \text{for } 1 \leq k \leq K-1 \\ \frac{K}{2} \psi \left( \frac{v}{K} \right), & \text{for } k = 0 \end{cases} \quad (11)$$

$$\mu_{\pm}(v) = \frac{1}{2} \left[ \psi \left( \frac{v}{K} \right) \pm \frac{v}{K} \right] \quad (12)$$

$$R = \begin{bmatrix} 1 & 1 & 1 \\ \frac{u}{2} & \frac{u^2}{2} + uc + \frac{c^2}{(\gamma-1)} & \frac{u^2}{2} - uc + \frac{c^2}{(\gamma-1)} \end{bmatrix} \quad (13)$$

$$R^{-1} = \begin{bmatrix} 1 - \frac{(\gamma-1)u^2}{2c^2} & (\gamma-1)\frac{u}{c^2} & -\frac{(\gamma-1)}{c^2} \\ -\frac{u}{2c} + \frac{(\gamma-1)u^2}{4c^2} & \frac{1}{2c} - \frac{(\gamma-1)u}{2c^2} & \frac{(\gamma-1)}{2c^2} \\ \frac{u}{2c} + \frac{(\gamma-1)u^2}{4c^2} & -\frac{1}{2c} - \frac{(\gamma-1)u}{2c^2} & \frac{(\gamma-1)}{2c^2} \end{bmatrix} \quad (14)$$

$$\tilde{g}_{i+\frac{1}{2}}^k = \sigma_{i+\frac{1}{2}}^k \alpha_{i+\frac{1}{2}}^k \quad (15)$$

$$g_i^k = \minmod\left(\tilde{g}_{i+\frac{1}{2}}^k, \tilde{g}_{i-\frac{1}{2}}^k\right) \quad (16)$$

Mathematical expressions of coefficient of numerical viscosity proposed by Roe, Lax-Wendroff and Harten are given in equations 17 to 20 respectively.

$$\psi(v) = |v| \quad (17)$$

$$\psi(v) = v^2 \quad (18)$$

$$\psi(v) = \begin{cases} \frac{1}{2}\left(\frac{v^2}{\varepsilon} + \varepsilon\right) & |v| < \varepsilon \\ |v| & |v| \geq \varepsilon \end{cases} \quad (19)$$

$$\psi(v) = v^2 + \frac{1}{4} \quad (20)$$

Table 1 shows the expressions for coefficient functions  $C_i(x)$  which were obtained after putting different values of  $K$  in equation 11.

**Table 1.**  $C_i(x)$  at different  $K$ .

$K$	$C_1$	$C_2$	$C_3$
2	$x^2$		
3	$x^2(3-x)$	$x^3$	
4	$x^2(6-4x+x^2)$	$2x^3(2-x)$	$x^4$

### 3. TEST CASE DESCRIPTION

Shock tube problem is used for validation purpose. SOD and Inverse Shock boundary conditions are used (Table 2). The size of computational domain is  $0 \leq x \leq 1$  and number of grid points are 1000. Entropy fix parameter  $\varepsilon$  is taken 0.1 while minmod limiter is used for all computations. Initial discontinuity centered on  $x = x_o$  and  $t = 0$  has following conditions:

$$U(x, t) = \begin{cases} U_L, & x < x_o \\ U_R, & x \geq x_o \end{cases} \quad \text{where, } x_o=0.5$$

**Table 2.** Boundary conditions for SOD and Inverse Shock cases.

Boundary conditions	$p_R$	$\rho_R$	$v_R$	$p_L$	$\rho_L$	$v_L$
SOD	0.1	0.125	0.0	1.0	1.0	0.0
Inverse Shock	1.0	1.0	5.91608	29.0	5.0	1.183206

#### 4. RESULTS AND DISCUSSION

In present work, Qian MLTS TVD scheme presented in equation (6) is studied with different entropy fix functions. Shock tube problem for SOD and Inverse Shock boundary conditions are solved to investigate the performance and behavior of MLTS TVD scheme with different entropy fix in the regions of expansion fan, discontinuities and strong shock waves.

The physical time for the flow processes are 0.15 and 0.05sec for SOD and Inverse Shock cases respectively. Simulations are carried out on Intel(R) Core(TM) 2, CPU @ 2.13 GHz, 2 GB RAM.

Fig. 1 to Fig. 5 show the density profile for SOD boundary conditions. Fig. 1 shows whole domain while Fig. 2 to Fig. 5 focus on start of expansion, end of expansion, contact, and shock regions respectively. Fig. 2 depicts that for lower values of CFL (0.9 and 1.9) the result with different entropy fix at the start of expansion fan is similar while for larger values of CFL (2.9 and 3.9) the result with entropy fix presented in equation 20 produces less dissipation. At the end of expansion fan minor oscillation is observed for equation 18 and equation 20, these oscillations grow up as K value increase, see Fig. 3(d). Results with entropy fix presented in equation 17 and 19 are more accurate as compare to other at the end of expansion fan location.

Investigation of Fig. 4 and Fig. 5 shows that the resolution for the contact discontinuity is captured worse than the shock wave for different entropy fix. The shock wave is a compressive wave and the characteristic lines are convergent so the dissipation near to the shock wave is controlled in a small level in the time marching steps. Near the contact wave the discrepancy of analytical and numerical results are worse for all entropy fix. Reason behind this is the fact that the contact discontinuity is a kind of linear wave in the theory of the hyperbolic conservation laws and the characteristic lines are parallel to each other so the dissipation can not be restrained. During the time marching step the dissipation is accumulated and the contact wave may span more and more grid points. Fig. 4 depicts that for lower values of CFL (0.9 and 1.9) the result with different entropy fix at contact is similar. For larger values of CFL (2.9 and 3.9) the result with entropy fix presented in equation 17 and equation 19 produces less dissipation and is non oscillatory while other two entropy fix produce oscillations.

Fig. 5 shows that for lower values of CFL (0.9 and 1.9) the result with different entropy fix at shock is similar. For larger values of CFL (2.9 and 3.9) the result with entropy fix presented in equation 18 and equation 20 produces less dissipation. Results near shock are oscillation free for all entropy fix used in present study. Fig. 6 to Fig. 10 show the density profile for Inverse Shock boundary conditions. Fig. 6 shows whole domain while Fig. 7 to Fig. 10 focus on start of expansion, end of expansion, contact, and shock regions, respectively. Fig. 6 depicts that for equations 17, 18 and 20 schemes does not have sufficient artificial viscosity for all CFL values and therefore nonphysical expansion shock is available in the result. This nonphysical behavior is due to the fact that the scheme with equations 17, 18 and 20 entropy fix cannot distinguish between an expansion shock and a compression shock. Both are valid result for this formulation.

Although scheme with entropy fix presented in equation 20 provide good result for smaller values of CFL however for larger CFL values (CFL = 3.9) this scheme become unstable and after some iteration it's blown up. Same is happened with scheme using entropy fix presented in equation 18. Schemes with entropy fix presented in equation 17 and equation 19 are found to be stable for all CFL values investigated in present studies.

It has been explored from Fig. 6 to Fig. 10 that scheme with entropy fix presented in equation 17 does not have sufficient artificial viscosity and produce nonphysical expansion shock for all CFL values investigated in present studies. Therefore scheme with entropy fix presented in equation 19 only produces real results without nonphysical expansion shock and stability issues.

It is summarized that for simple cases all entropy fix provide physical results with minor oscillation and dissipation issues for all CFL values investigated in present studies. However for complex test cases, like inverse shock boundary condition, only Harten's derived entropy fix (equation 19) is stable and depict physical behavior precisely for LTS TVD.

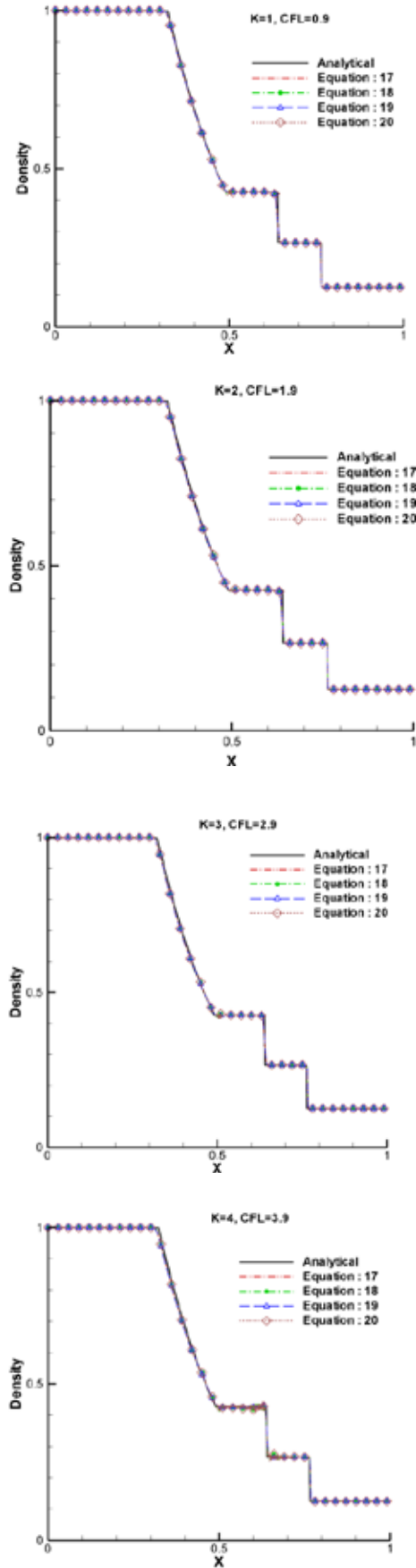


Fig. 1. Overall density profile, SOD case.

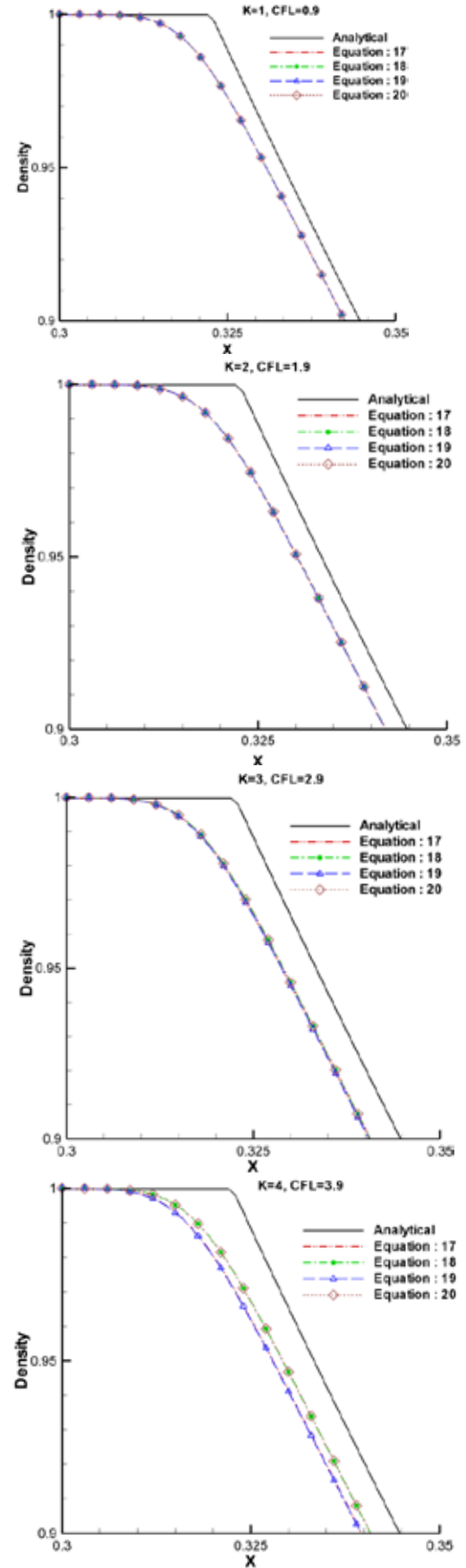


Fig. 2. Start of expansion, SOD case.

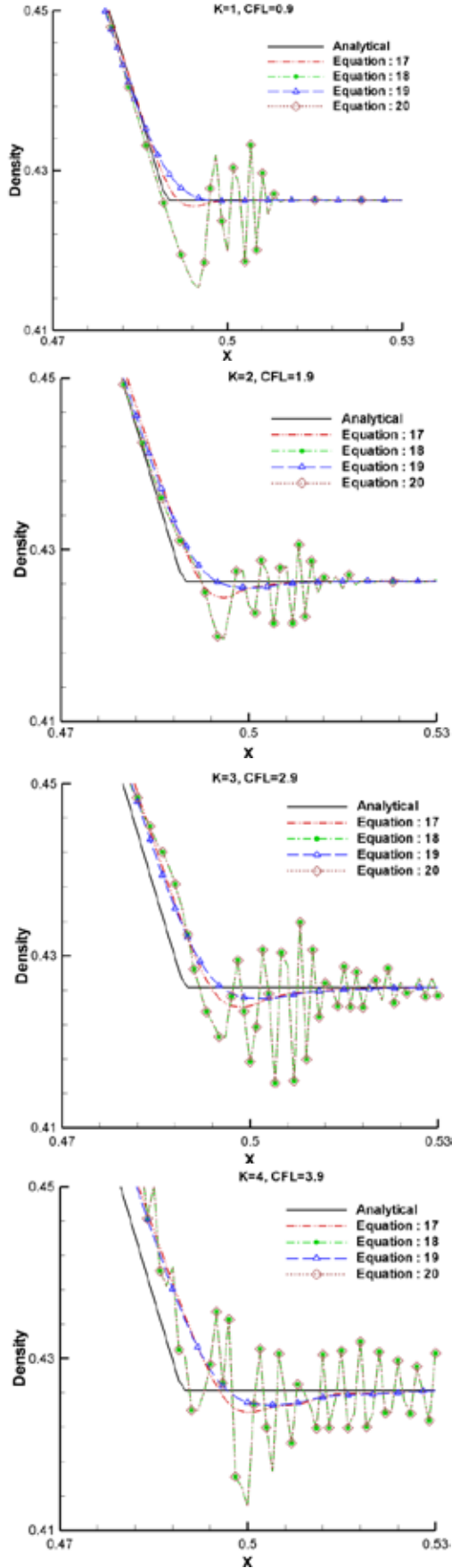


Fig. 3. End of expansion, SOD case.

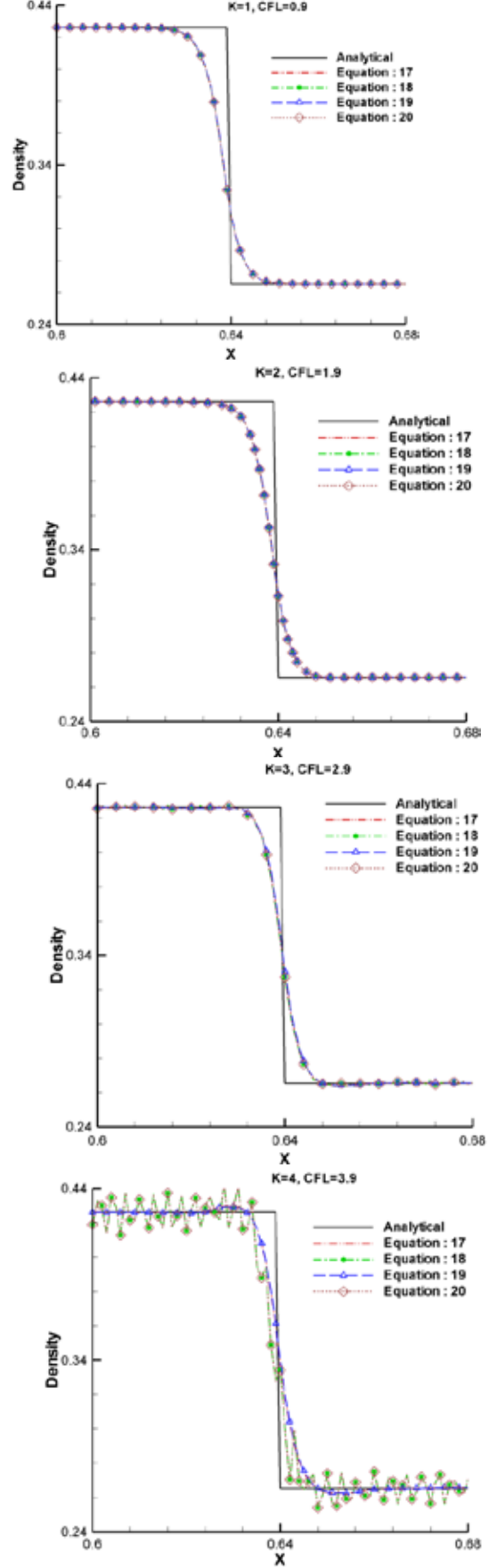


Fig. 4. Contact region, SOD case.

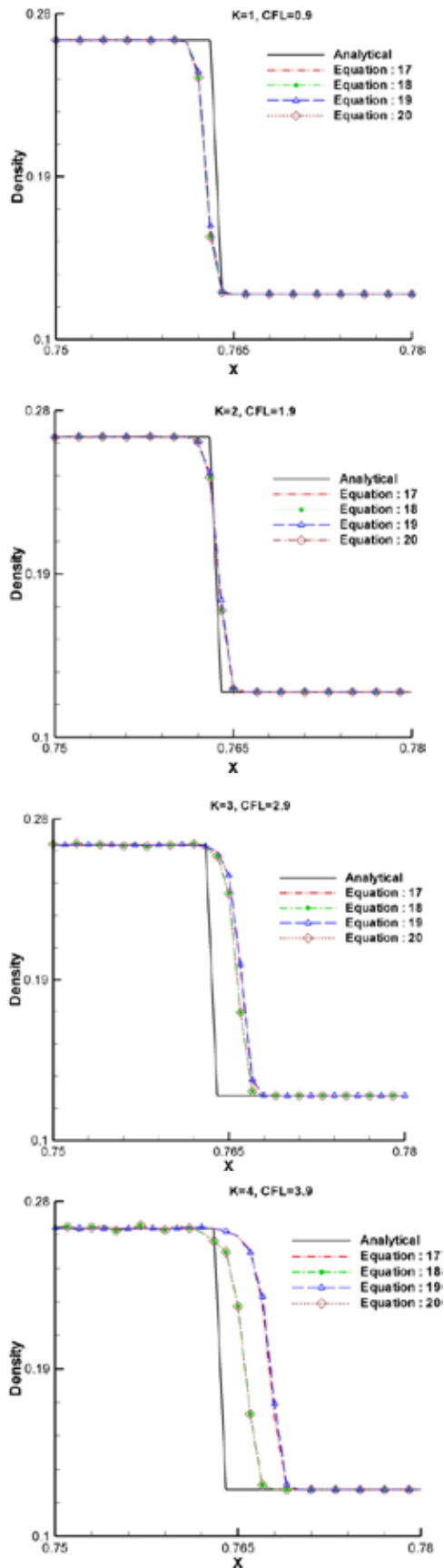


Fig. 5. Shock region, SOD case.

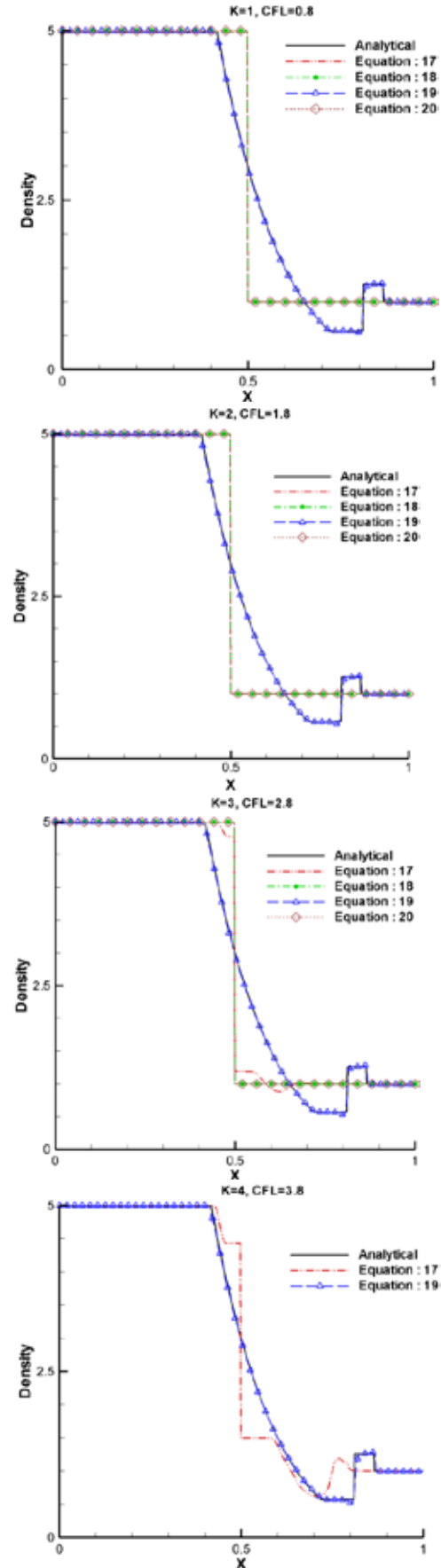


Fig. 6. Overall profiles, inverse shock. Case.



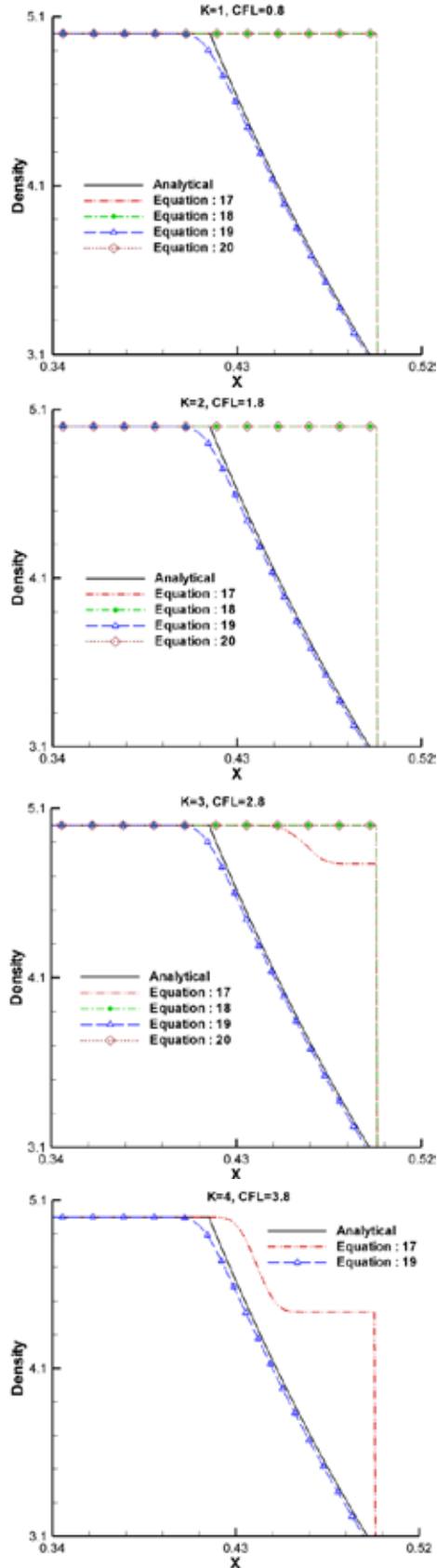


Fig. 7. Start of expansion, inverse shock case.

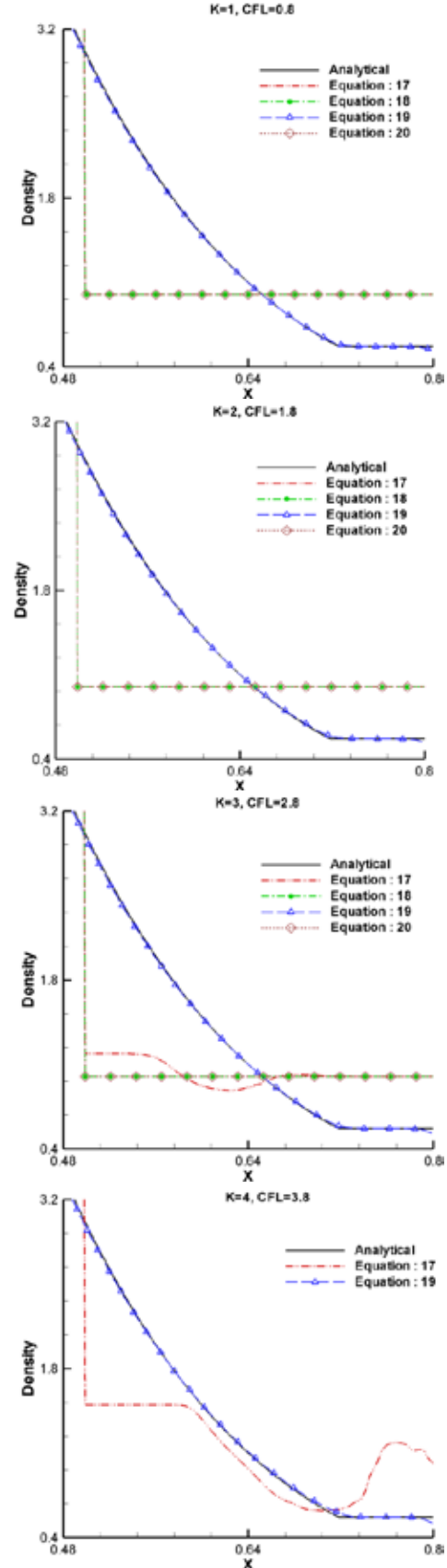


Fig 8: End of expansion, inverse shock case.

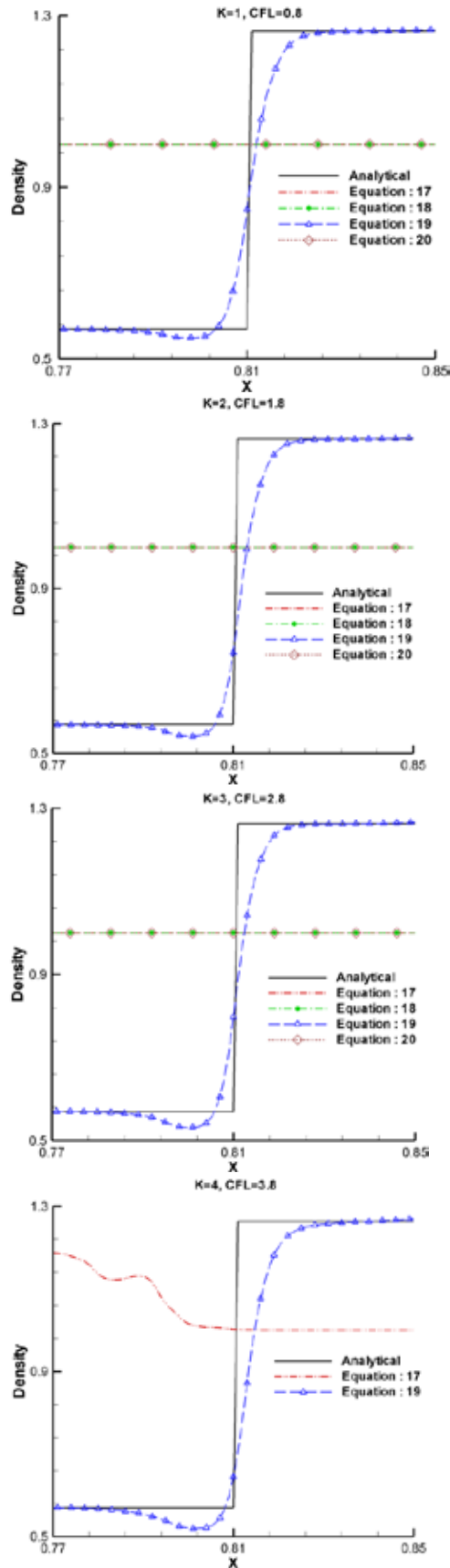


Fig. 9: Contact region, inverse shock case.

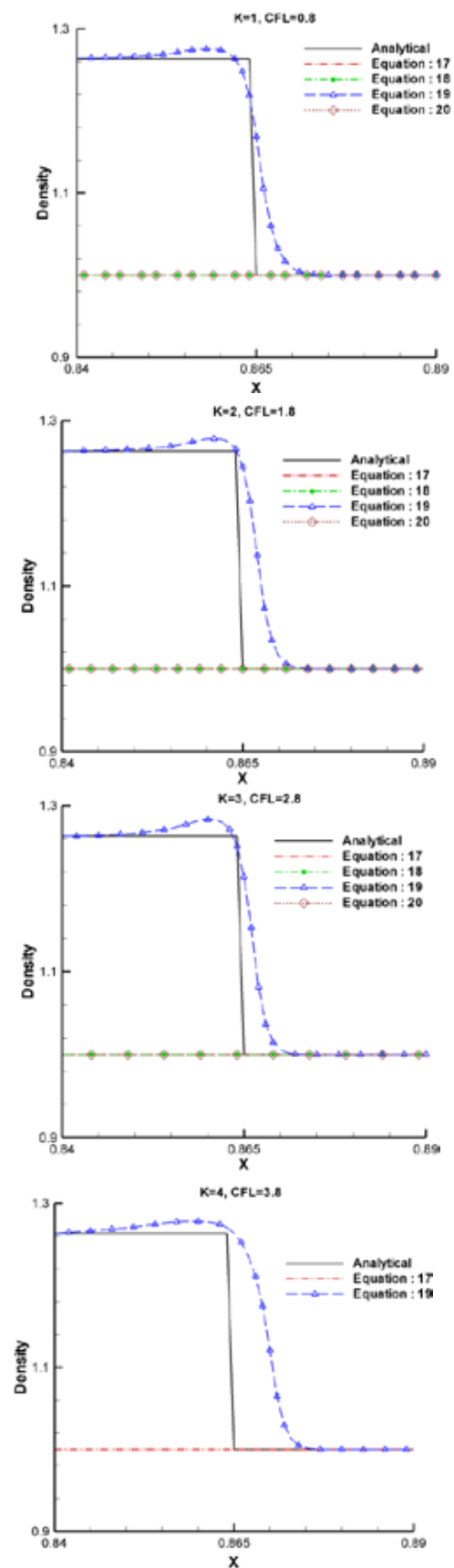


Fig. 10: Shock region, inverse shock case.

## 5. CONCLUSIONS

In present work LTS TVD scheme developed by Harten and improved by Qian have been investigated for different entropy fix conditions. Computed results are analyzed for merits and shortcomings of different entropy fix with large time step schemes. Shock tube problem is used for validation purpose. It is concluded that for simple cases all entropy fix provide physical results with minor oscillation and dissipation issues for all CFL values investigated in present studies. However for complex test cases, like inverse shock boundary condition, only Harten's derived entropy fix is stable and depicts physical behavior precisely for LTS TVD.

In the present work the numerical results were computed for 1D shock tube problem only. Similar studies must be pursued for more complex 2D and 3D flows in future. Large time step scheme behavior with different entropy fix for various Eigen vector matrix and flux limiter should also be investigated.

## NOMENCLATURE

$A$	inviscid flux jacobion matrix	$n$	number of time steps taken
$C_{l(x)}$	coefficient functions	$p$	pressure
$C_{k(v)}$	entropy fixing function	$t$	time
$E$	total energy	$\Delta t$	time step
$F$	physical flux	$u$	velocity in x-direction
$K$	CFL restriction parameter	$v$	local CFL number
$R$	eigen vector matrix	$x$	axial distance
$R^{-1}$	inverse eigen vector matrix	$\Delta x$	grid spacing
$U$	conservative variable vector	$\alpha$	characteristic variable
$a$	characteristic speed	$\beta$	numerical characteristic speed
$c$	speed of sound	$\varepsilon$	entropy fix parameter
$f$	numerical flux	$\Phi$	numerical dissipation term
$g$	flux correction	$\gamma$	ratio of specific heat
$\tilde{g}$	limiter function	$\lambda$	mesh ratio
$i$	grid points	$\mu$	CFL parameter
$k$	characteristic direction	$\rho$	density
$m$	number of eigen values	$\sigma$	limiter function parameter
		$\psi$	entropy correction function

## 6. REFERENCES

1. Harten, A. The artificial compression method for computation of shocks and contact discontinuities: III. Self-adjusting hybrid schemes. *Mathematics of Computation* 32 (142): 363-389 (1978).
2. Harten, A. High resolution schemes for hyperbolic conservation laws. *Journal of Computational Physics* 135: 260-278 (1997).
3. Harten, A. On a Large time-step high resolution scheme. *Mathematics of Computation* 46(174): 379-399 (1986).
4. Hoffmann, K., & S. Chiang. *Computational Fluid Dynamics. Engineering Education System (EES)*, 4<sup>th</sup> ed., Vol I. Wichita, Kansas, USA (2000).
5. Hoffmann, K., & S. Chiang. *Computational Fluid Dynamics. Engineering Education System (EES)*, 4<sup>th</sup> ed., Volume II. Wichita, Kansas, USA (2000).
6. Huang, H., C. Leey, H. Dongz, & J. Zhang. Modification and applications of a large time-step high resolution TVD scheme. In: *51st AIAA Aerospace Sciences Meeting including the New Horizons Forum and Aerospace Exposition, AIAA*, p. 2013-2077 (2013).
7. John, D., & J. Anderson. *Computational Fluid Dynamics: The Basics with Applications*. McGraw-Hill, USA (1976).
8. Laney, C. *Computational Gasdynamics*. Cambridge University Press, New York, USA, (1998).
9. Lax, P.D. *Hyperbolic Systems of Conservation Laws and the Mathematical Theory of Shock Waves*. SIAM, New York (1973).
10. Mukkarum, H., U.H. Ithram, & F. Noor. Efficient and accurate scheme for hyperbolic conservation laws. *International Journal of Mathematical Models and Methods in Applied Sciences*, NUAN 9: 504-511 (2015).
11. Noor, F., & H. Mukkarum. To study large time step high resolution low dissipative schemes for hyperbolic conservation laws. *Journal of Applied Fluid Mechanics*, vol. 9 (2016).

12. Roe, P. Approximate Riemann solvers, parameter vectors, and difference schemes. *Journal of Computational Physics* 43: 357-372 (1981).
13. SOD, G.A. A survey of several finite difference methods for systems of nonlinear hyperbolic conservation laws. *Journal of Computational Physics* 27 (1978).
14. Sweby, P.K. High resolution schemes using flux limiters for hyperbolic conservation laws. *Journal on Numerical Analysis*, SIAM 21(5): 995-1011 (1984).
15. Tannehill, J., D. Anderson, & H. Pletcher. *Computational Fluid Mechanics and Heat Transfer*, 2nd ed. Taylor & Francis, CA, USA (1984).
16. Toro, E.F. *Riemann Solvers and Numerical Methods for Fluid Dynamics: A Practical Introduction*, 3<sup>rd</sup> ed., Springer, Berlin (2009).
17. Versteeg, H., & W. Malalasekera. *An Introduction to Computational Fluid Dynamics: The Finite Volume Method*, 2<sup>nd</sup> ed. Pearson Prentice Hall, England, United Kingdom (2007).
18. Yee, H. *Upwind and Symmetric Shock-Capturing Schemes*. NASA Technical Memorandum 130: 89464 (1987).
19. Yee, H.C. *A Class of High-Resolution Explicit and Implicit Shock-Capturing Methods*. Ames Research Center, NASA Technical Memorandum 101088 , 228., Moffett Field, CA, USA (February 1989).
20. Yee, H., G. Klopfer, & J. Montagn. *High-Resolution Shock-Capturing Schemes for Inviscid and Viscous Hypersonic Flows*. NASA Technical Memorandum 100097, 38. USA (April 1988).
21. Yee, H., N. Sandham, & M. Djomehri. Low dissipative high order shock capturing methods using characteristic based filter. *Journal of Computational Physics* 150: 199-238 (1999).
22. ZhanSen, Q.C.L. A class of large time step godunov scheme for hyperbolic conservation laws and applications. *Journal of Computational Physics* 230: 7418-7440 (2011).
23. ZhanSen, Q.C.-H.L. On large time step tvd scheme for hyperbolic conservation laws and its efficiency evaluation. *Journal of Computational Physics* 231: 7415-7430 (2012).